POLAR STRATIGRAPHY FROM HIRISE STEREO TOPOGRAPHY. P. Becerra[1], S. Byrne[1], S. Mattson[1], J.D. Pelletier[2], K.E. Herkenhoff[3], and the HiRISE Science Team[1]. [1]Lunar and Planetary Laboratory, University of Arizona, Tucson, AZ, USA. becerra@lpl.arizona.edu. [2]Department of Geosciences, University of Arizona, Tucson, AZ, USA [3]U.S. Geological Survey, Flagstaff, AZ, USA.

Introduction: The North and South Polar Layered Deposits (NPLD and SPLD) of Mars are broad sheets of water ice and dust that make up the bulk of the martian polar caps. They have been eroded by canyons that allow a view of their underlying stratigraphy (fig. 1), which is composed of many depositional layers of varying thicknesses that are thought to represent a record of recent climate change on Mars [1].

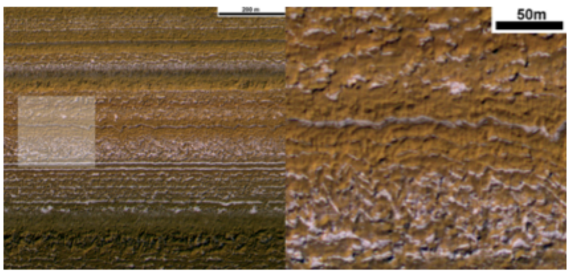

Fig. 1. HiRISE PSP_001738_2670. Left: Layer exposures on a scarp on the NPLD. Right: Blow-up of highlighted area showing slumping lag deposits.

Deciphering this record is one of the most important unresolved issues in Mars polar science [2]. Several researchers have approached this question by attempting to extract a periodic climate signal from stratigraphic sequences constructed from images of the PLD scarps [1-7]. This type of analysis is similar to those applied to ice cores extracted from Earth's major ice sheets. The majority of these investigations created virtual ice cores of the NPLD by plotting layer albedo from MOC images versus depth taken from MOLA data [3,4,6]. These studies generally agree that there is a dominant stratigraphic wavelength of 25 – 30 m in the upper 300 m of the NPLD. Although wavelet analysis by [6] found little evidence for this signal, they found a possible dominant wavelength at 1.6 m.

Exact co-registration of the MOC and MOLA data is an issue that may be circumvented by using HiRISE stereo topography and orthorectifying the input images. Using HiRISE stereo pairs, Limaye et al. [7] performed Fourier analysis on brightness and slope for NPLD and SPLD sites. They confirmed a 1.6 m signal for the NPLD and found no periodicity in the SPLD.

The major weakness of the previously mentioned studies was the use of albedo as the mapped layer property. The brightness of exposed PLD layers is a complicated product of slopes, frost retention, albedo and surface texture. In addition, it is now known that a sublimation lag deposit mantles these exposures (fig. 1, right) [8]. So it is not clear how brightness relates to properties of the layers themselves, if at all.

Recent work used high-resolution images and Digital Terrain Models (DTMs) from HiRISE to map morphological properties of discrete layers within a sequence [2, 7]. Fishbaugh et al. [2] created the first high resolution stratigraphic column of the NPLD based entirely on morphological properties, categorizing layers into marker beds and thin layer sets based on texture and apparent protrusion from adjacent materials on the wall. The authors likely identified the structures responsible for both the 30 m and the 1.6 m signals. Limaye et al. [7] made similar stratigraphic columns based on bed thickness and provided the first high-resolution stratigraphic mapping of SPLD layers. The disadvantage of discrete layer mapping is that there are no continuous depth-varying quantities that could be examined with spectral analysis tools.

In this study we seek to expand upon this work by examining depth-varying properties that have previously not been studied, using more advanced spectral analysis, and creating new HiRISE DTMs and orthorectified images to examine a widespread area of both PLDs. Initially, we use a measure of how the protrusion of layers from the scarp face varies with depth (extracted from DTMs), which can be taken as a proxy for a layer's resistance to erosion [9].

Data and Analysis: Using 1 m/pixel HiRISE DTMs, we can create linear profiles of layer protrusion to be examined with spectral analysis methods [9]. An example DTM profile, along with a schematic of the method to extract layer protrusion is shown in fig. 2.

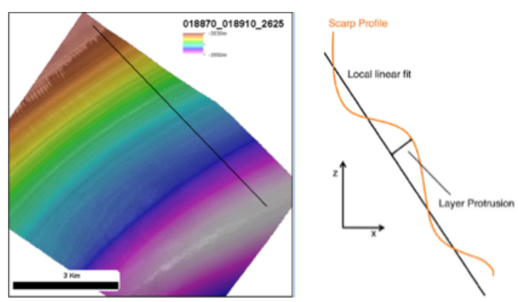

Fig. 2. Left: HiRISE DTM displaying NPLD layers at 82N 34 E. Right: Schematic of the calculation of layer protrusion from the local (~ 100 m) scarp-face.

A profile is extracted from the DTM in the downhill direction. The small-scale structure is quantified with a "sliding window" along the profile in which the best-fit linear trend is evaluated. The protrusion is then computed by calculating the difference between the actual topography and the window center. This procedure allows for the creation of a continuous profile of layer protrusion vs. depth along the scarp.

We identified 11 sites on the NPLD and 4 sites on the SPLD with completed DTMs (fig. 3). In addition, we plan to create more DTM's from available HiRISE stereo pairs, as well as acquire new targets in order to achieve as much geographical coverage as possible. Our approach is to calculate five protrusion profiles from different areas of one DTM, which can be compared to each other in order to identify individual layers from different sections of one scarp. This will help the construction of more accurate stratigraphic columns from each DTM, and will make it easier to identify and correlate these layers in other DTMs taken from different regions of the PLD. Three of the protrusion profiles calculated from the DTM from fig. 2 are shown in fig. 4 (these have not yet been adjusted to line up in elevation). We have extracted five protrusion profiles from all available DTMs with exposed layers.

Byrne et al. [9] performed wavelet analysis on protrusion profiles of NPLD exposures at five locations, and found a common dominant wavelength in the stratigraphy of ~40-45 m, as well as multiple secondary signals. The wavelet power spectrum of one of the protrusion profiles from the left panel of fig. 4 is plotted as a function of elevation and wavelength on the right panel of fig. 4. The advantage of wavelet analysis is that it can quantify signals that change in periodicity with depth [10]. We will use this method to examine all of selected sites from both polar caps.

Discussion and Future Work: There are many complications in deducing the relationship between the stratigraphy of the PLDs and Martian climate. The cratering record of the SPLD indicates that it is much older than the NPLD [11,12], meaning they might contain records of two very different periods in Martian climate, and a relationship between the two might not be clearly present. Although the variations of orbital elements that could force climate change on Mars are now reasonably well known for the past 10-20 Myrs, the climate itself, and the polar accumulation and erosion rates are not well constrained. In addition, many of the exposed stratigraphic sequences contain unconformities that break the record and make the detection of a periodic signal much more complicated.

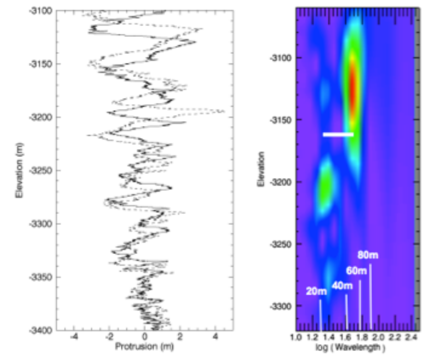

Fig. 4. Left: 3 protrusion profiles taken from the DTM shown in fig. 2 (NPLD 1). Right: Wavelet power spectrum (using a Morlet basis) of the solid profile form the left, as a function of wavelength and position.

Hvidberg et al. [13] made considerable progress by constructing a model of layer formation that expresses polar deposition rates of ice and dust in terms of insolation, and comparing it to the stratigraphic column constructed by Fishbaugh et al. [2]. In their model, dust-rich layers form by increased summer sublimation during high obliquity, and by variations in the polar deposition of dust regulated by obliquity changes. Their results date the top 500 m of the NPLD at 1 Myr with an average net deposition rate of ice and dust of 0.55 mm/yr.

Our primary objective is to analyze new DTMs with more advanced methods, focusing on the SPLD. Ultimately, we wish to develop a model similar to that of [11] with which we can evaluate the relationship between PLD stratigraphy and climate evolution.

References: [1] Cutts, JGR 78 (1973). [2] Fishbaugh et al., GRL 37 (2010). [3] Laskar et al., Nature 419 (2002). [4] Milkovich and Head, JGR 110 (2005). [5] Fishbaugh and Hvidberg, JGR 111 (2006). [6] Perron and Huybers, Geology 37 (2009). [7] Limaye et al., JGR 117 (2012). [8] Herkenhoff et al. Science, 317 (2007). [9] Byrne et al., V Mars Polar Sci. Conf. (2011). [10] Torrence and Compo, Bull. Am. Met. Soc. 79 (1998). [11] Herkenhoff and Plaut, Icarus 144 (2000). [12] Koutnik et al., JGR 107 (2002). [13] Hvidberg et al., Icarus, 221 (2012).

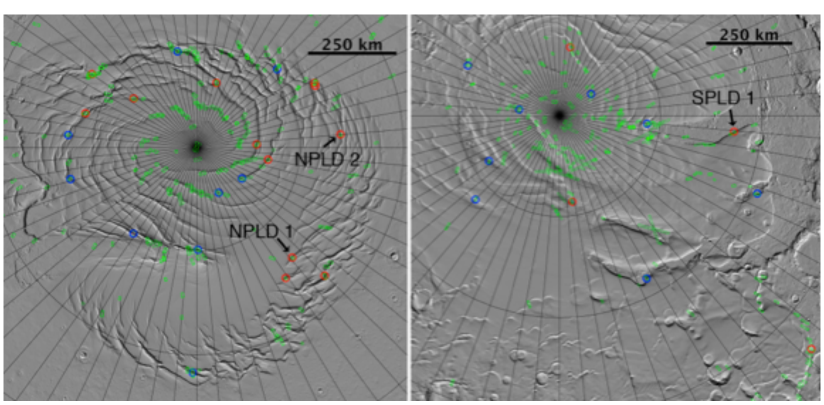

Fig. 3. Map of available and future DTMs (Left: NPLD, Right: SPLD). The green stamps represent available HiRISE stereo observations. Red circles indicate the locations of currently available DTMs. Blue circles indicate locations where we plan to create the next DTMs for this study.